Supporting Information

The Supporting Information is available free of charge (PDF). Table containing energy-dispersive X-ray spectroscopy microanalysis data. Figures showing X-ray microCT, thermogravimetric analysis, X-ray powder diffraction, Fourier-Transform Infrared spectroscopy, Transmission Electron Microscopy.

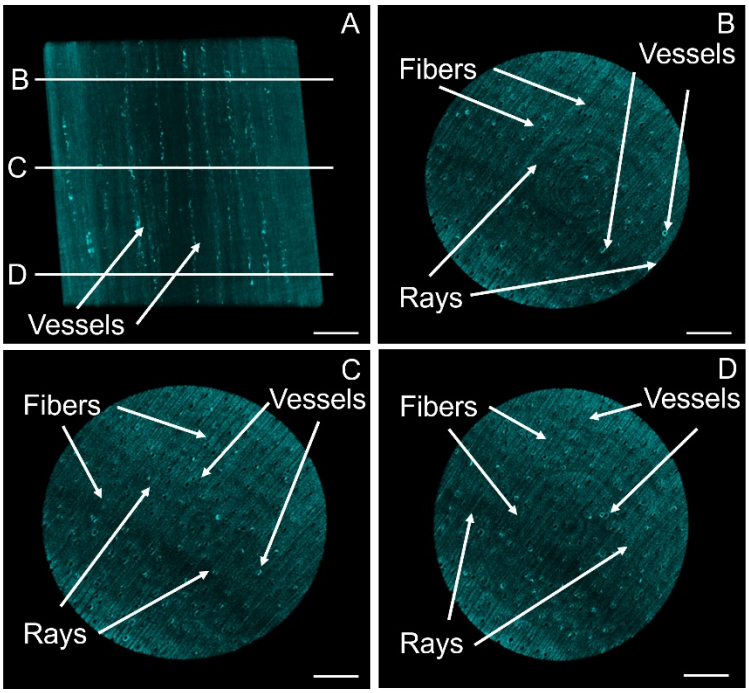

Figure S1. MicroCT of Mt mineralized composite showing distribution of Fe within the lignocellulose scaffold. A) slice in the axial direction showing Mt distribution primarily at the interface of vessels of the wood structure. B,C,D) radial slices showing Mt at different heights of the filter.

	C [Wt%]	O [Wt%]	K [Wt%]	Fe [Wt%]	Pt [Wt%]	Ca [Wt%]
P1	60.7±0.2	13.7±0.1	12.7±0.1	11.6±0.1	0.8±0.1	0.5±0
P2	56.4±0.2	21.6±0.2	16.7±0.1	5.3±0.1	N/A	N/A
P3	58.6±0.2	21.9±0.1	10.8±0.1	8.3±0.1	N/A	0.3±0
P4	54.7±0.1	23.9±0.1	10.7±0	9.0±0	1.1±0	0.6±0
P5	65.9±0.1	19.3±0.1	5.5±0	8.1±0	1.2±0	N/A
P6	51.0±0.2	10.4±0.1	20.8±0.1	15.3±0.1	1.1±0.1	1.4±0

Table S1. SEM/EDS point analyses from Fh-modified cell walls.

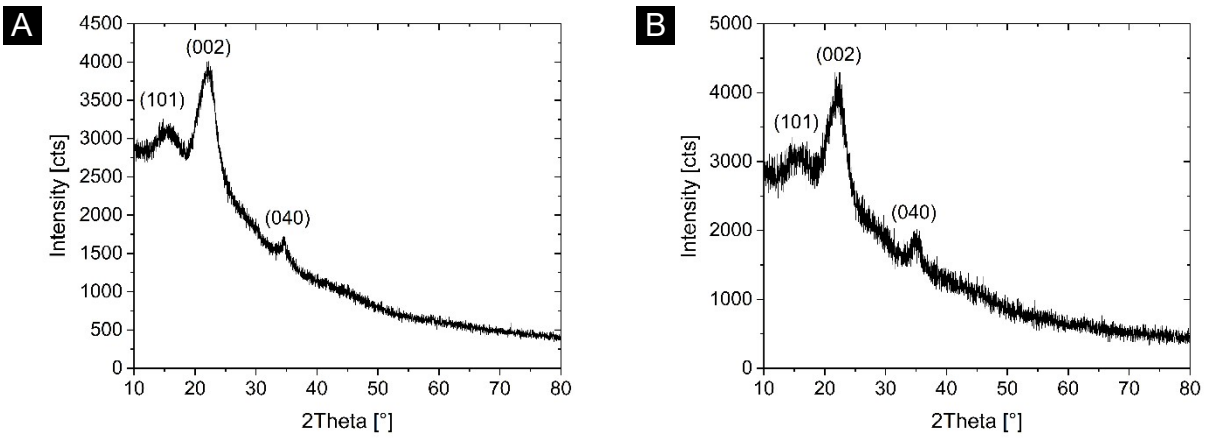

Figure S2. Powder X-Ray diffraction of wood composite materials with ferrihydrite **(A)** and magnetite **(B)**. Pronounced Bragg reflections from the semicrystalline cellulose I_β in balsa wood overshadow the XRD peaks from the mineral phases. Miller indices of cellulose are shown on each respective plot.

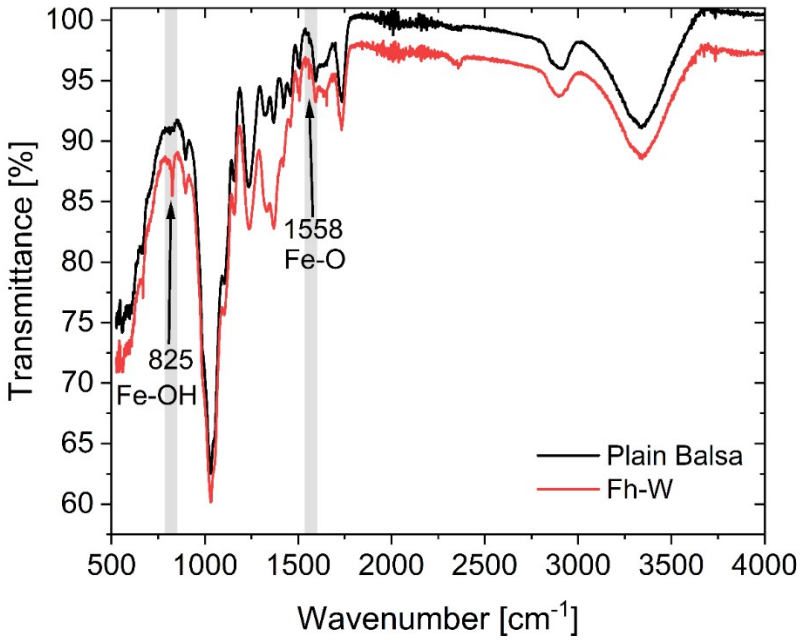

Figure S3. FT-IR spectra of balsa wood before and after modification with ferrihydrite. Bands attributed Fe-OH bending (825cm^{-1}) and Fe-O stretching (1558cm^{-1}) are characteristic of 2-line ferrihydrite.

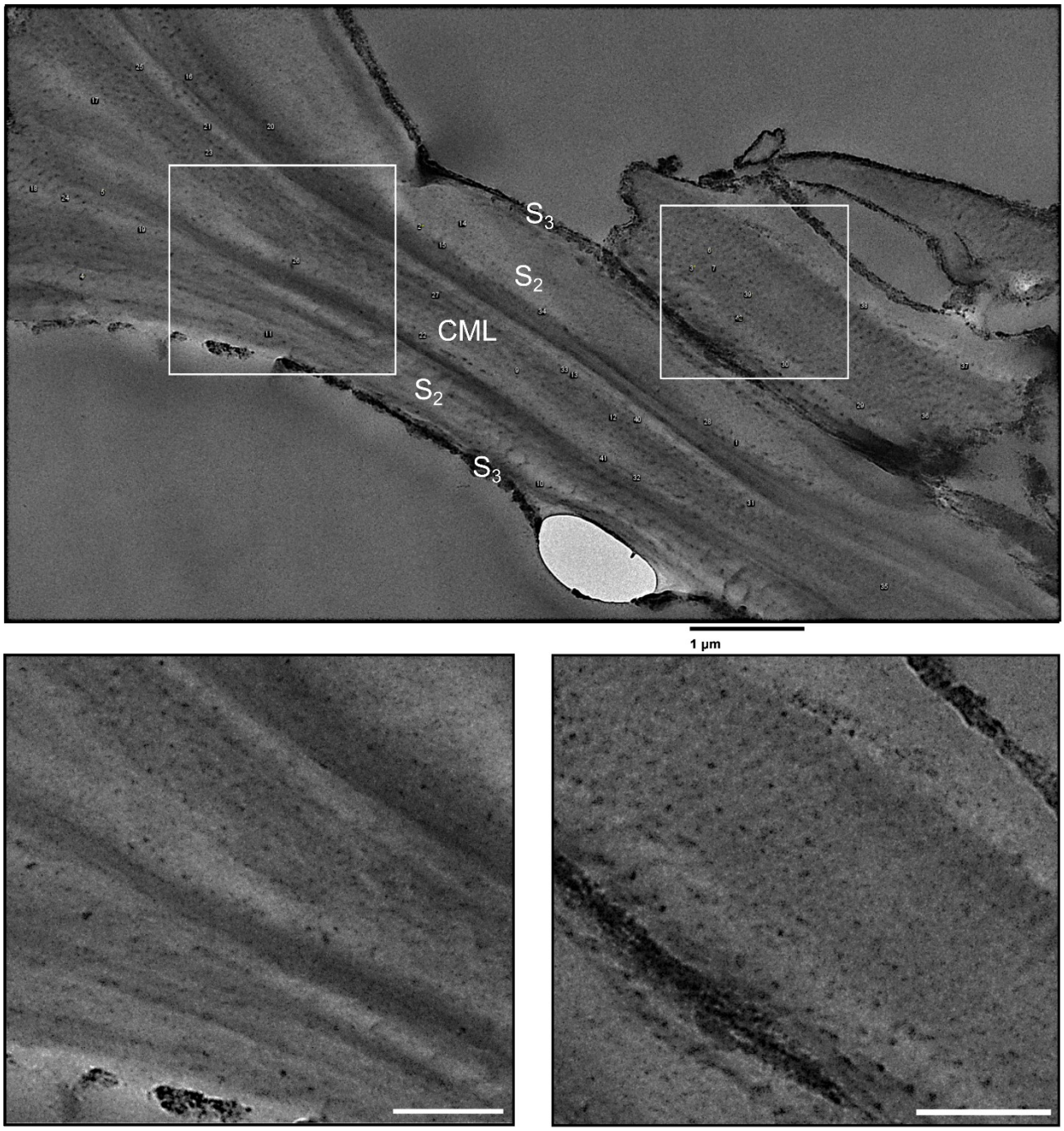

Figure S4. Transmission Electron Micrograph shows formation of nanocrystalline Fh particles within compound middle lamella (CML), S1, and S2 cell wall layers and at S3 cell wall/lumen interface. Scale bar corresponds to 1µm. Numbers indicate location of measured Fh particles. The results of the size measurements are given in Table S1. Magnified TEM micrographs show Fh nanoparticles with an average size of 27±6 nm within the wood cell wall. Scalebars equal 500nm.

No.	Particle size [nm]	No.	Particle size [nm]
1	31	22	24
2	32	23	25
3	26	24	32
4	32	25	24
5	32	26	23
6	44	27	30
7	29	28	34
8	22	29	23
9	35	30	28
10	17	31	15
11	26	32	33
12	27	33	27
13	30	34	35
14	30	35	26
15	23	36	21
16	21	37	25
17	25	38	29
18	29	39	25
19	20	40	30
20	26	41	19
21	31	42	18

Table S2. Particle sizes from TEM micrograph (Fig. S4) measured with ImageJ.

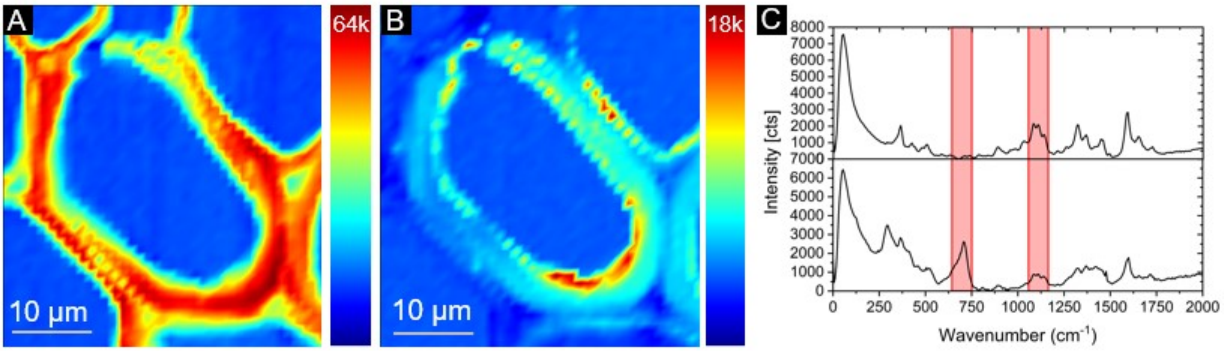

Figure S5. Confocal Raman analysis of Mt modified balsa. Chemical mappings of individual fibers were plotted to show distribution of Mt |650-750 cm^{-1}| (A) with respect to the cellulose in the wood cell structure |1100-1200 cm^{-1}| (B). Raman spectra from the red regions of interest in the respective images were averaged and plotted to show the strong magnetite peak at ~700 cm^{-1} (lower curve) in the lumen that is absent within the cell wall (upper curve) (C).

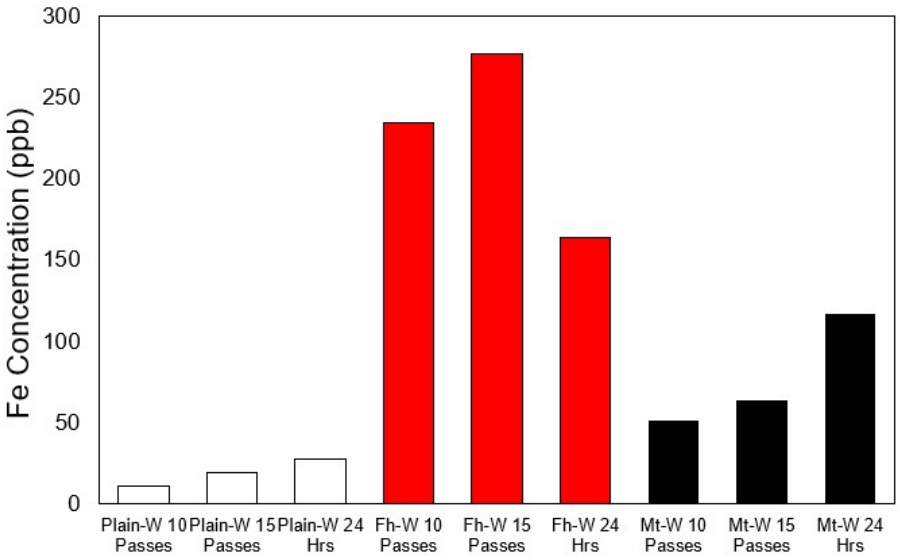

Figure S6. Plot of Fe values from ICP-MS data obtained from 100 µg/L As solution after treatment with filters to measure amount of Fe leaching. None of the measured Fe concentrations exceeded the EPA limit of 300 µg L^{-1} (=300 ppb) drinking water.

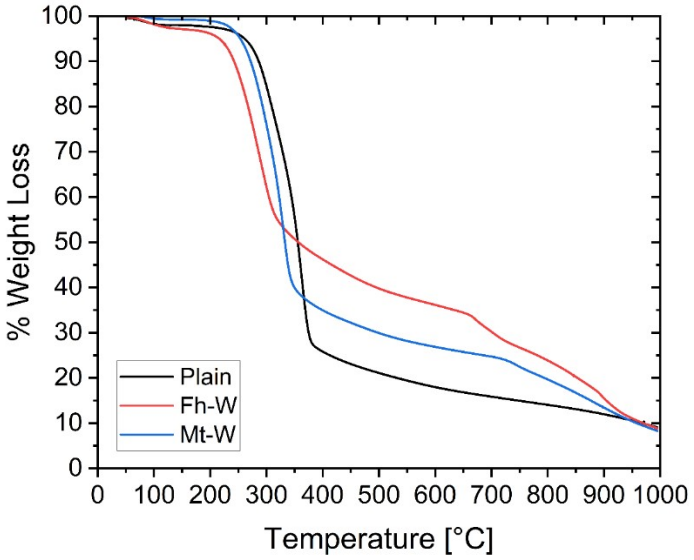

Figure S7. Thermogravimetric analysis of powdered balsa and composite material. Comparison of remaining weight percents at 300-400° C can be used to estimate and compare the mineralized content of the materials.